

# Resonance Raman scattering and *ab initio* calculation of electron energy loss spectra of MoS<sub>2</sub> nanosheets

**Anirban Chakraborti**

School of Computational & Integrative Sciences, Jawaharlal Nehru University, New Delhi-110067, India

E-mail: anirban@jnu.ac.in

**Arun Singh Patel**

School of Computational & Integrative Sciences, Jawaharlal Nehru University, New Delhi-110067, India

E-mail: arunspatel.jnu@gmail.com

**Pawan K. Kanaujia**

Nanophotonics Laboratory, Department of Physics, Indian Institute of Technology Delhi, New Delhi-110016, India

E-mail: kanaujiapk09@gmail.com

**Palash Nath**

Department of Physics, University of Calcutta, 92 APC Road, Kolkata-700009, India

E-mail: palashnath20@gmail.com

**G.Vijaya Prakash**

Nanophotonics Laboratory, Department of Physics, Indian Institute of Technology Delhi, New Delhi-110016, India

E-mail: prakash@physics.iitd.ernet.in

**Dirtha Sanyal**

Variable Energy Cyclotron Centre, 1/AF Bidhannagar, Kolkata-700064, India

E-mail: dirtha@vecc.gov.in

**Abstract.** The presence of electron energy loss (EELS) peak is proposed theoretically in molybdenum disulfide (MoS<sub>2</sub>) nanosheets. Using density functional theory simulations and calculations, one EELS peak is identified in the visible energy range, for MoS<sub>2</sub> nanosheets with molybdenum vacancy. Experimentally, four different laser sources are used for the Raman scattering study of MoS<sub>2</sub> nanosheets, which show two distinct Raman peaks, one at 385 cm<sup>-1</sup> ( $E_{2g}^1$ ) and the other at 408 cm<sup>-1</sup> ( $A_{1g}$ ). In

the cases of three laser sources with wavelengths 405 nm (3.06 eV), 632 nm (1.96 eV) and 785 nm (1.58 eV), respectively, the intensity of  $E_{2g}^1$  Raman peak is more than the  $A_{1g}$  Raman peak, while in the case of excitation source of 532 nm (2.33 eV), the intensity profile is reversed and  $A_{1g}$  peak is the most intense. Thus a resonance Raman scattering phenomenon is observed for 532 nm laser source.

PACS numbers: 62.23.Kn, 78.67.-n

*Keywords:* MoS<sub>2</sub>, Density functional theory, electron energy loss, Raman scattering

## 1. Introduction

The discovery of graphene in 2004 provided a novel way of studying two dimensional layered structure materials [1, 2, 3, 4, 5, 6, 7]. In the recent few years, it has been possible to synthesize different kind of two dimensional nanomaterials of metal chalcogenides, in which d-electrons' interactions can give rise to new physical phenomena. Among these materials, the transition-metal dichalcogenide semiconductor MoS<sub>2</sub> has attracted special attention, as it exhibits intriguing properties [8, 9, 10, 11, 12, 13]. Bulk MoS<sub>2</sub> is composed of covalently bonded S-Mo-S sheets that are bound by weak van der Waals forces and is an indirect band gap semiconductor with band gap of the order of 1.2 eV. However, a single layer of MoS<sub>2</sub> is a direct band gap semiconductor with a band gap of 1.9 eV [14, 15]. This band gap lies in the visible range and the work function of MoS<sub>2</sub> is compatible with the commonly used electrode materials. Moreover, the single layer of MoS<sub>2</sub> is fluorescent in nature with having quantum yield of the order of 10<sup>4</sup> more than the bulk MoS<sub>2</sub> [16]. Thus MoS<sub>2</sub> has potential applications in electronic, optoelectronic and photonic devices [16, 2, 17]. For example, the field effect transistors based on MoS<sub>2</sub> show high on/off switching ratio, [15] which is of the order of 10<sup>8</sup>.

There are numerous studies on the intriguing properties and broad applications of MoS<sub>2</sub> nanosheets; only recently, a study by Bruno et al. reported the resonance Raman scattering in MoS<sub>2</sub> nanosheets [18]. Conventionally, the EELS spectroscopy can be used to find out the band gap in semiconducting materials. It has been studied that the doping in semiconductors causes tuning in the band gap of these materials. In this work, we have studied the effect of different kinds of vacancies (Mo, S) in the EELS spectra of MoS<sub>2</sub> nanosheets, and attempt has been made to correlated theoretical results of EELS with the Raman spectroscopic study. For the first time we have tried to correlate the theoretical results of EELS to the Raman spectroscopic results. It is found that molybdenum vacancy in MoS<sub>2</sub> nanosheets shows a EELS peak around 2.4 eV and Raman spectroscopic study shows enhancement of A<sub>1g</sub> peak at 532 nm laser excitation source, thus a resonance Raman scattering phenomenon is observed at 2.3 eV excitation source.

## 2. Methods

### 2.1. Computational methods

For the theoretical modeling and density functional theory (DFT) calculations, we have used the Vienna Ab Initio Simulation (VASP) code, [19, 20, 21, 22] along with the MedeA software package. Before the evaluation of frequency dependent dielectric properties, all the structures were geometrically relaxed until the unbalanced force components converge below 0.02 eV/Å. Simulations were performed under the generalized gradient approximation (GGA) with Perdew-Burke-Ernzerhof (PBE) exchange and correlation [23, 24]. A mesh cutoff energy of 400 eV, has been set in the expansion of plane wave basis sets and the electronic ground state convergence criteria has been set by 10<sup>-5</sup> eV for

all the systems. The Brillouin zone (BZ) has been sampled by  $7 \times 7 \times 1$  Monkhorst-Pack (MP) grid point [25]. Electron energy loss spectra (EELS) of pristine MoS<sub>2</sub> system, MoS<sub>2</sub> system with sulfur vacancy and MoS<sub>2</sub> system with molybdenum vacancy have been explored in the framework of density functional theory (DFT).

## 2.2. Experimental methods

The proposed theoretical model is supported by Raman spectroscopic study of MoS<sub>2</sub> sheets. The MoS<sub>2</sub> nanosheets were prepared by chemical exfoliation method [26]. For this purpose, 1 g of bulk MoS<sub>2</sub> powder was mixed with 1 mL of N-Methyl-2-pyrrolidone (NMP) and the mixture was ground for 30 min in mortar pestle. The paste like mixture was put in vacuum oven at room temperature over night. The mixture was redispersed into 20 mL of NMP solvent and ultra-sonicated for 10 h using 25 W ultrasonication bath. After ultrasonication, the mixture was centrifuged to separate out the MoS<sub>2</sub> nanosheets. The supernatant was collected from the solution which contained MoS<sub>2</sub> nanosheets. Such obtained dispersion of MoS<sub>2</sub> sheets were drop cast on silicon substrate and annealed above 220 °C for Raman and scanning electron microscopic (SEM) studies. For transmission electron microscopic (TEM) analysis the solution was put on carbon coated copper grid and dried at room temperature.

## 3. Results and discussion

### 3.1. DFT calculation

In DFT calculations, first the frequency dependent dielectric function ( $\epsilon(\omega)$ ) of a system has been computed; then electron energy loss spectra (EELS) of this system has been evaluated using the relation:  $L(\omega) = \text{Im}(-1/\epsilon(\omega))$ . From EELS (see figure 1) it is identified that the spectrum shows asymmetrical nature in between two polarization states of electromagnetic (EM) wave; which is the manifestation of layered structure of MoS<sub>2</sub>. The results for the electronic energy loss spectra for MoS<sub>2</sub> nanosheets are shown in figure 1.

Pristine MoS<sub>2</sub> system does not exhibit any significant loss peak in the visible range below 3.0 eV optical frequency. Besides, defect induced systems such as MoS<sub>2</sub> with sulfur vacancy as well as MoS<sub>2</sub> with molybdenum vacancy both demonstrate the existence of low energy loss peak in the visible part. Atomic vacancy induces localization of electron density near the vacancy site that actually gives rise to new plasmon excitations in the visible range as observed from EELS. One of the interesting features observed from EELS is that the emergence of new loss peaks in the infrared to visible part at 0.4 eV and 2.48 eV optical frequency for perpendicular polarization ( $E_{\perp}$ ) in case of molybdenum vacancy system (see figure 1 (c)). Besides, there exists no signature of such loss peaks in case of  $E_{\perp}$  polarization in both pristine and sulfur vacancy system.

Since MoS<sub>2</sub> nanosheet is a two dimensional material with a layered structure, the in-plane (X-Y plane) symmetries are different from the out of plane (perpendicular

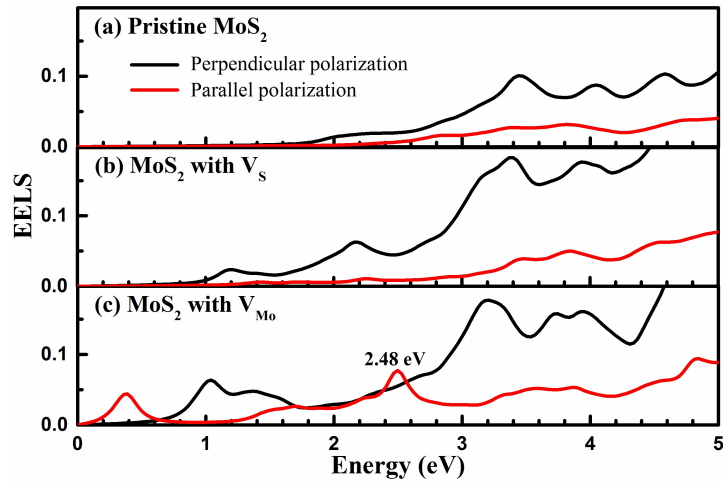


**Figure 1.** Electron energy loss spectra of (a) pristine MoS<sub>2</sub> nanosheets, (b) MoS<sub>2</sub> nanosheets with sulfur vacancy ( $V_S$ ) and (c) MoS<sub>2</sub> nanosheets with molybdenum vacancy ( $V_{Mo}$ ). The black line denotes perpendicular polarization and the red line denotes parallel polarization.

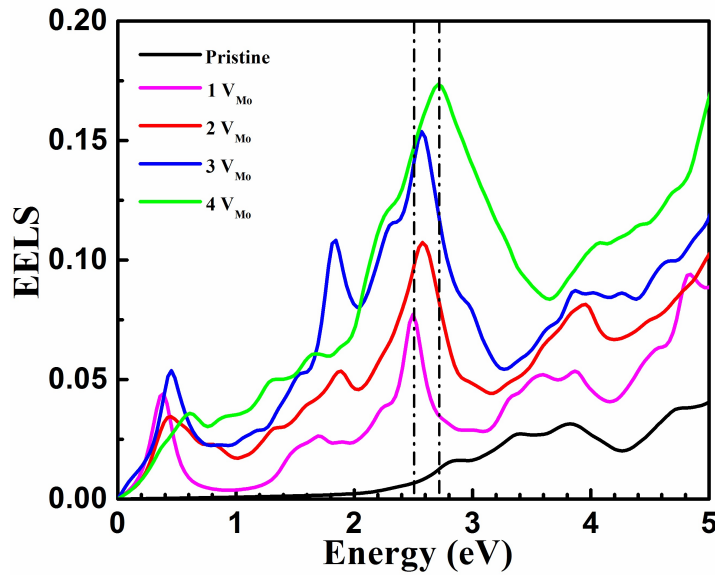


**Figure 2.** Electron energy loss spectra of MoS<sub>2</sub> nanosheets with varying concentrations of molybdenum vacancy ( $V_{Mo}$ ). The black line denotes parallel polarization for pristine MoS<sub>2</sub>. A single molybdenum vacancy ( $1V_{Mo}$ ) is depicted by the magenta line;  $2V_{Mo}$  by red,  $3V_{Mo}$  by blue, and  $4V_{Mo}$  by green, respectively.

direction) symmetries. Thus, the associated chemical bonding and electron distribution is different along the perpendicular direction compared to the in-plane direction, which results in formation of two different excitation modes in the in-plane direction and perpendicular plane direction of the MoS<sub>2</sub> nanosheet. In general, they occur at different excitation energies also. The presence of  $V_{Mo}$  in the structure gives rise to electron localization at the vacancy site, on the MoS<sub>2</sub> layer. These localized electrons result in a distinct, out-of-plane excitation peak (or EELS peak) at  $\sim 2.5$  eV energy. Note that

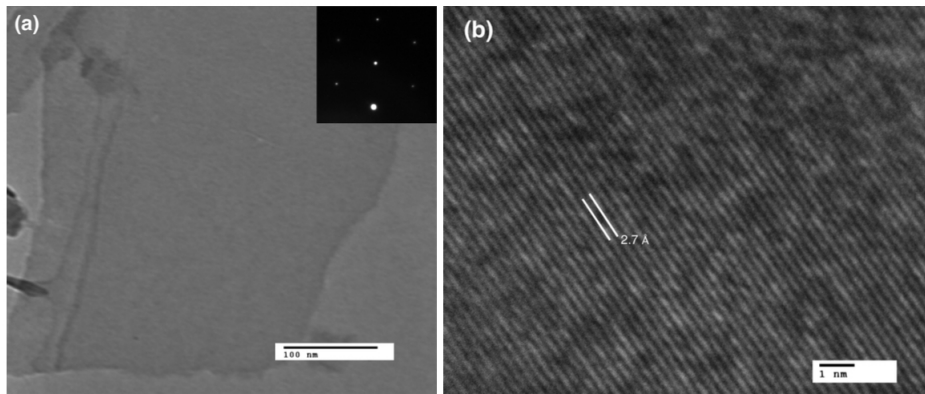


**Figure 3.** TEM images of (a) MoS<sub>2</sub> nanosheets, with inset showing SAED pattern (scale equals to 100 nm); (b) lattice spacing in MoS<sub>2</sub> nanosheet (scale equals 1 nm).

no excitation peak exists at the similar energy in case of in-plane plasma oscillation. To confirm the existence of the EELS peak at  $\sim 2.5$  eV energy, DFT calculations were performed for several systems having various molybdenum vacancies  $V_{\text{Mo}}$  or defect concentrations. Interestingly, it is noted that the increase of vacancy concentration enhances the EELS peak height (see figure 2). Moreover, a little blue shift of the peak position is observed with increasing defect concentration, although the shift does not affect the final results and conclusions of this present observation.

### 3.2. TEM analysis

Presence of sheets like structure in MoS<sub>2</sub> was confirmed by transmission electron microscope image analysis. The TEM images were obtained by a transmission electron microscope (model JEOL-2100F, Japan), operating at 200 kV. The TEM image of MoS<sub>2</sub> nanosheets is shown in figure 3.

The inset of figure 3(a) shows the selective area electron diffraction (SAED) pattern from MoS<sub>2</sub> nanosheet. Figure 3(b) shows the lattice spacing in MoS<sub>2</sub> nanosheet. The lattice spacing between adjacent planes is of the order of 2.7 Å which corresponds to (100) plane.

### 3.3. SEM analysis

The SEM image of MoS<sub>2</sub> nanosheets was recorded by scanning electron microscope (Zeiss EVO40). The sheets like structure of MoS<sub>2</sub> was observed in the scanning electron microscopy. The SEM image of MoS<sub>2</sub> nanosheets is shown in figure 4. The size of these nanosheets are of order of 10  $\mu\text{m}$ .

### 3.4. Raman spectroscopic study

The Raman spectra of MoS<sub>2</sub> were collected by Renishaw inVia confocal Raman spectrometer using four different excitation laser sources 405 nm, 532 nm, 632 nm and

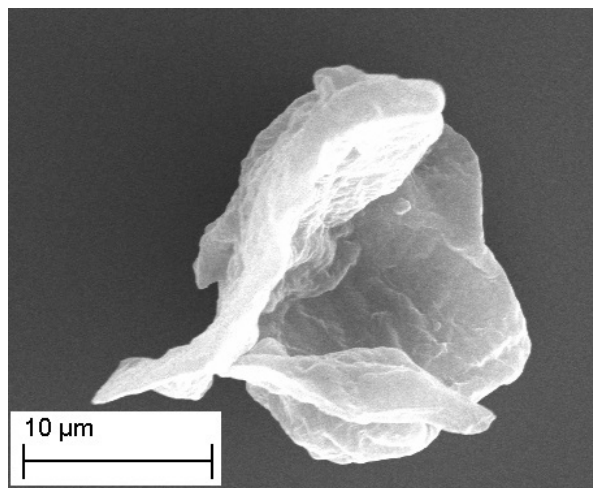


**Figure 4.** SEM image of MoS<sub>2</sub> nanosheets.

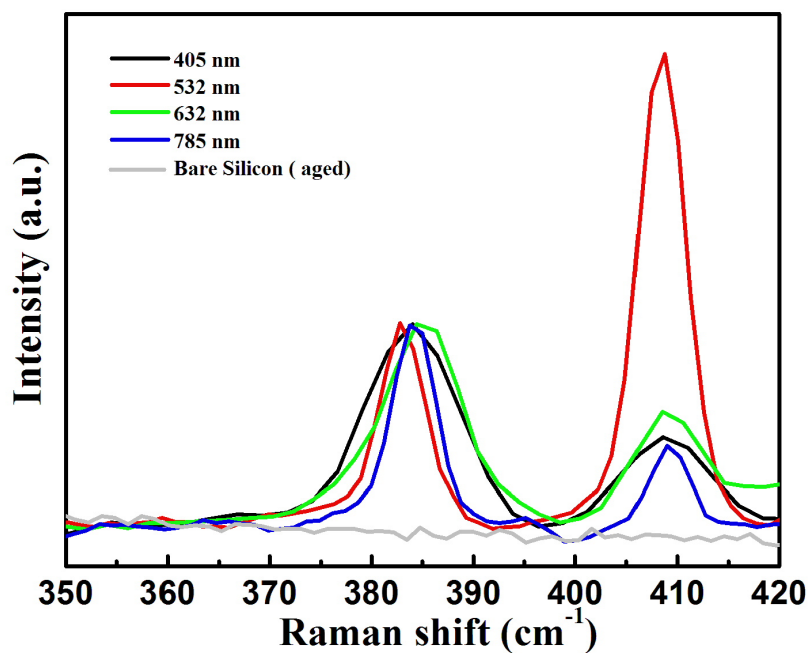


**Figure 5.** Raman spectra of MoS<sub>2</sub> nanosheets for different laser excitation sources: 405 nm (3.06 eV), 532 nm (2.33 eV), 632 nm (1.96 eV) and 785 nm (1.58 eV). The Raman spectrum of bare silicon (aged) is plotted in grey.

785 nm. For 405 nm and 532 nm lasers the associated grating is 2400 lines per mm while for 632 nm and 785 nm lasers it is 1200 lines per mm. The Raman spectra were collected by using 50X objective lens having numerical aperture 0.25.

Figure 5 shows the Raman spectra of MoS<sub>2</sub> nanosheets. The spectra consist two Raman peaks one at 385 cm<sup>-1</sup> and other at 408 cm<sup>-1</sup>. The Raman peak at 385 cm<sup>-1</sup> is known as  $E_{2g}^1$  peak and other at 408 cm<sup>-1</sup> is  $A_{1g}$  peak, these peaks originate due to in

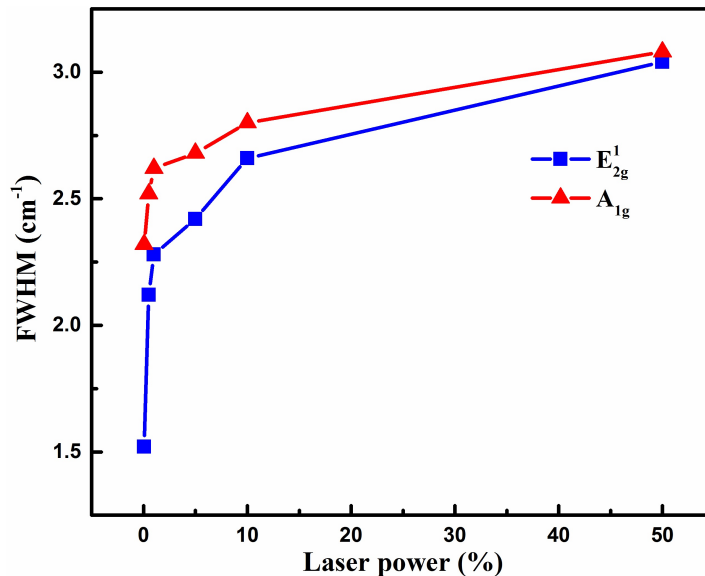


**Figure 6.** Effect of laser (532 nm) power on the full width half maximum (FWHM) of  $E_{2g}^1$  and  $A_{1g}$  peaks of MoS<sub>2</sub> nanosheets.

plane and out of plane vibrations of S-Mo-S bonds. The effect of excitation source on the Raman peaks of MoS<sub>2</sub> nanosheets has been analyzed. For all three wavelengths of laser sources, 405 nm (3.06 eV), 632 nm (1.96 eV) and 785 nm (1.58 eV) the intensity of  $E_{2g}^1$  peak is greater than the intensity of  $A_{1g}$  peak while in case of 532 nm (2.33 eV) excitation source the intensity of  $A_{1g}$  is more than that of the  $E_{2g}^1$  peak. Our theoretical analysis shows that an EELS peak is observed around 2.48 eV. Hence the enhancement of the Raman peak is due to the resonance occurring at 532 nm.

In order to verify whether the intensity enhancement of  $A_{1g}$  Raman peak under 532 nm laser excitation, comes from the Si/SiO<sub>2</sub> substrate, we tested the Raman response in the bare area of the sample (without the MoS<sub>2</sub>) to see Si/SiO<sub>2</sub> substrate. Here, we have used aged Si, since it may have more native SiO<sub>2</sub>. As evident from figure 5, there is no conflict of SiO<sub>2</sub> Raman peaks within the region of MoS<sub>2</sub> peaks and the intensity enhancement of the  $A_{1g}$  peak (identified at 2.48 eV in the visible range for MoS<sub>2</sub> nanosheet with molybdenum vacancy) comes from a resonance Raman scattering, and certainly not from the Si/SiO<sub>2</sub> substrate.

The effect of laser power on the full width half maximum (FWHM) of both the peaks have been studied using 532 nm laser source (figure 6). With increase in the power of laser the FWHM value of  $E_{2g}^1$  and  $A_{1g}$  peaks increases and attains a saturation level.

#### 4. Conclusions

In summary, we have demonstrated the presence of EELS peak in molybdenum disulfide (MoS<sub>2</sub>) nanosheets in the visible energy range. Theoretically, using DFT simulations



and calculations, an EELS peak was identified at 2.48 eV (visible range), for MoS<sub>2</sub> nanosheets with molybdenum vacancy; for pristine MoS<sub>2</sub> and MoS<sub>2</sub> with sulfur vacancy, the EELS did not show any resonance peaks for parallel polarization. This was then confirmed experimentally, using four different laser sources for the Raman scattering study of MoS<sub>2</sub> nanosheets. In the cases of three laser sources with wavelengths 405 nm (3.06 eV), 632 nm (1.96 eV) and 785 nm (1.58 eV), respectively, the intensity of  $E_{2g}^1$  Raman peak was more than the  $A_{1g}$  Raman peak, while in the case of excitation source of 532 nm (2.33 eV), the intensity profile was reversed and  $A_{1g}$  peak was the most intense. Such a resonance phenomena may trigger some new features such as generation of localized energy states. The presented 2D nanosheets have a great potential for future optical systems, especially in nanophotonic devices operating at visible wavelengths.

## Acknowledgement

AC acknowledges the financial support by institutional research funding IUT (IUT39-1) of the Estonian Ministry of Education and Research. AC and ASP acknowledge financial support from grant number BT/BI/03/004/2003(C) of Government of India, Ministry of Science and Technology, Department of Biotechnology, Bioinformatics division. Authors thank the AIRF, JNU for TEM and SEM characterizations and the FIST (DST, Govt. of India) UFO scheme of IIT Delhi for Raman/PL facility.

## References

- [1] Novoselov K S, Geim A K, Morozov S, Jiang D, Zhang Y, Dubonos S, Grigorieva I and Firsov A 2004 *Science* **306** 666–669
- [2] Mak K F, Lee C, Hone J, Shan J and Heinz T F 2010 *Phys. Rev. Lett.* **105** 136805
- [3] Radisavljevic B, Radenovic A, Brivio J, Giacometti V and Kis A 2011 *Nat. Nanotechnol.* **6** 147–150
- [4] Kibsgaard J, Chen Z, Reinecke B N and Jaramillo T F 2012 *Nat. Mater.* **11** 963–969
- [5] Nath P, Chowdhury S, Sanyal D and Jana D 2014 *Carbon* **73** 275 – 282 ISSN 0008-6223 URL <http://www.sciencedirect.com/science/article/pii/S000862231400205X>
- [6] Lin J, Li H, Zhang H and Chen W 2013 *Appl. Phys. Lett.* **102** 203109
- [7] Shakya J, Patel A S, Singh F and Mohanty T 2016 *Appl. Phys. Lett.* **108** 013103
- [8] Prins F, Goodman A J and Tisdale W A 2014 *Nano Lett.* **14** 6087–6091
- [9] Wang Y, Ou J Z, Balendhran S, Chrimes A F, Mortazavi M, Yao D D, Field M R, Latham K, Bansal V, Friend J R *et al.* 2013 *ACS Nano* **7** 10083–10093
- [10] Ou J Z, Chrimes A F, Wang Y, Tang S y, Strano M S and Kalantar-zadeh K 2014 *Nano Lett.* **14** 857–863
- [11] Castellanos-Gomez A, Poot M, Steele G A, van der Zant H S, Agrait N and Rubio-Bollinger G 2012 *Adv. Mater.* **24** 772–775
- [12] Miwa J A, Ulstrup S, Sørensen S G, Dendzik M, Čabo A G c v a c, Bianchi M, Lauritsen J V and Hofmann P 2015 *Phys. Rev. Lett.* **114**(4) 046802 URL <http://link.aps.org/doi/10.1103/PhysRevLett.114.046802>
- [13] Zheng Y, Chen J, Ng M F, Xu H, Liu Y P, Li A, O’Shea S J, Dumitrică T and Loh K P 2015 *Phys. Rev. Lett.* **114**(6) 065501 URL <http://link.aps.org/doi/10.1103/PhysRevLett.114.065501>
- [14] Ganatra R and Zhang Q 2014 *ACS Nano* **8** 4074–4099
- [15] Sreeprasad T, Nguyen P, Kim N and Berry V 2013 *Nano Lett.* **13** 4434–4441

- [16] Splendiani A, Sun L, Zhang Y, Li T, Kim J, Chim C Y, Galli G and Wang F 2010 *Nano Lett.* **10** 1271–1275
- [17] Wang R, Ruzicka B A, Kumar N, Bellus M Z, Chiu H Y and Zhao H 2012 *Phys. Rev. B* **86**(4) 045406 URL <http://link.aps.org/doi/10.1103/PhysRevB.86.045406>
- [18] Carvalho B R, Malard L M, Alves J M, Fantini C and Pimenta M A 2015 *Phys. Rev. Lett.* **114**(13) 136403 URL <http://link.aps.org/doi/10.1103/PhysRevLett.114.136403>
- [19] Kresse G and Hafner J 1993 *Phys. Rev. B* **47** 558
- [20] Kresse G and Hafner J 1994 *Phys. Rev. B* **49**(20) 14251–14269 URL <http://link.aps.org/doi/10.1103/PhysRevB.49.14251>
- [21] Kresse G and Furthmüller J 1996 *Comput. Mater. Sci.* **6** 15–50
- [22] Kresse G and Furthmüller J 1996 *Phys. Rev. B* **54**(16) 11169–11186 URL <http://link.aps.org/doi/10.1103/PhysRevB.54.11169>
- [23] Perdew J P, Burke K and Ernzerhof M 1996 *Phys. Rev. Lett.* **77**(18) 3865–3868 URL <http://link.aps.org/doi/10.1103/PhysRevLett.77.3865>
- [24] Perdew J P, Burke K and Ernzerhof M 1997 *Phys. Rev. Lett.* **78**(7) 1396–1396 URL <http://link.aps.org/doi/10.1103/PhysRevLett.78.1396>
- [25] Monkhorst H J and Pack J D 1976 *Phys. Rev. B* **13**(12) 5188–5192 URL <http://link.aps.org/doi/10.1103/PhysRevB.13.5188>
- [26] Wang Y, Ou J Z, Chrimes A, Carey B, Daeneke T, Alsaif M M A, Mortazavi M, Zhuiykov S, Medhekar N V, Bhaskaran M *et al.* 2015 *Nano Lett.* **15** 883–890